

1 **Operational soil moisture data assimilation for improved continental water balance**
2 **prediction**

3
4

5 Siyuan Tian^{1*}, Luigi J. Renzullo¹, Robert C. Pipunic², Julien Lerat², Wendy Sharples², Chantal
6 Donnelly²

7 ¹ Fenner School of Environment & Society, The Australian National University, ACT, 2601, Australia

8 ² Water Program, Bureau of Meteorology, Australia

9

10 Corresponding author: Siyuan Tian (siyuan.tian@anu.edu.au)

11

12 **Key Points:**

- 13 • We develop a simple and efficient method to improve operational soil water balance
14 model through satellite data assimilation.
- 15 • We suggest an approach to use analyzed surface soil moisture estimates to impart mass
16 conservation constraints on related states and fluxes
- 17 • The impact of the satellite data assimilation on model estimates of soil moisture can
18 persist for several weeks.

19

20

21

22

23 **Abstract**

24 A simple and efficient method was developed to improve soil moisture representation in an
25 operational water balance model through satellite data assimilation. The proposed method
26 exploits temporal covariance statistics between modelled and satellite-derived soil moisture to
27 produce analysed estimates, as a weighted combination of all data sources. We demonstrate the
28 application of the method to the Australian Water Resources Assessment (AWRA) model and
29 evaluate the accuracy of the approach against in-situ observations across the water balance. The
30 correlation between simulated surface soil moisture and in-situ observation is increased from
31 0.54 (open-loop) to 0.77 (data assimilation). We suggest an approach to use analysed surface
32 moisture estimates to impart mass conservation constraints on related states and fluxes of the
33 AWRA model in a post-analysis adjustment. The improvements gained from data assimilation
34 can persist for more than one week in surface soil moisture estimates and one month in root-zone
35 soil moisture estimates.

36

37 **Plain Language Summary**

38 The access to accurate daily continental soil water balance predictions is valuable for water
39 management practitioners, policy makers and researchers in support of water resources
40 assessment and agriculture planning. This study develops a simple and robust method for an
41 operational water balance model to incorporate satellite soil moisture products for improved
42 accuracy and spatial representation of soil water storage predictions. The integration of satellite
43 soil moisture products can provide persistent constraints in model predictions for up to several
44 weeks.

45

46 **1 Introduction**

47 Accurate estimation of soil moisture is fundamental to monitoring and forecasting water
48 availability and land surface conditions under extreme events such as droughts, heatwaves and
49 floods (Ines et al., 2013; Sheffield and Wood, 2007; Tian et al., 2019a; Wanders et al., 2013).
50 The assimilation of satellite soil moisture into land surface and hydrology models has been
51 repeatedly demonstrated to improve model representation of soil water dynamics (Draper et al.,
52 2012; Kumar et al., 2009; Pipunic et al., 2008; Reichle and Koster, 2005; Renzullo et al., 2014;
53 Tian et al., 2017; Tian et al., 2019b). Soil moisture is the linchpin between atmospheric fluxes,
54 surface- and ground-water hydrology, thus it is important that any changes in modelled estimates
55 are not detrimental to other components of the water balance.

56 Soil moisture anomalies can persist for months (Vinnikov et al., 1996), but the spatial pattern can
57 vary significantly due to the heterogeneous spatial distribution of rainfall and variability in soil
58 properties, land cover type and topography. Due to this large spatial variability of soil moisture,
59 the utility of ground-based, point-scale measurements is limited. Soil moisture estimates from
60 land surface models are adversely affected by the uncertainties of atmospheric forcing, model
61 dynamics and model parameterization. Remotely sensed data can provide spatially and
62 temporally varying constraints on the modelling of biophysical landscape variables that are often
63 superior to that achieved by a single static set of model parameters. Data assimilation merges
64 models and observations in a way that compensates for the deficiencies in each (e.g. uncertainty,
65 coverage), resulting in improved accuracy, coverage, and ultimately forecasting capability.

66 Methods of assimilation are many and varied, however commonalities exist between them. These
67 commonalities are such, that for any time step, the time integrated first guess (the forecast) of
68 soil moisture states are adjusted by an amount determined by the difference between observed
69 and modelled soil moisture (the innovation), which is weighted by the respective error variances
70 of modelled and observed quantities (the gain), to generate revised soil moisture states (the
71 analysis). At this point, the model soil moisture states are out of balance with the other stores and

72 fluxes, until the model integrates forward to the next time step, whereupon water balance is
73 restored through model physics.

74 In addition to water balance closure, from an operational perspective, is it important that the
75 method of data assimilation be: computationally efficient for routine, automated simulation over
76 the whole model domain; robust to data gaps; and make lasting positive improvements to future
77 predictions of soil water stores and fluxes. Currently, there are very few operational continental
78 land surface modelling systems that provide high-resolution near-real time soil moisture
79 estimates that have been constrained through the assimilation of satellite observations. Some
80 recent examples include surface soil wetness observations from Advanced Scatterometer
81 (ASCAT) active radar system, on the meteorological operational satellite (MetOp), been
82 assimilated into Unified Model (Davies et al., 2005) through nudging to provide soil moisture
83 analysis at 40 km globally (Dharssi et al., 2011). Additionally, ASCAT data are used in the
84 ECMWF (European Centre for Medium-Range Weather Forecasts) Land Data Assimilation
85 System through a simplified Extended Kalman Filter approach (De Rosnay et al., 2013) to
86 provide near-real time surface soil moisture and root-zone soil moisture at 25-km resolution
87 globally. However, soil moisture products from a passive radiometer system such as SMOS (Soil
88 Moisture and Ocean Salinity) mission (Kerr et al., 2001) or the SMAP mission (Entekhabi et al.,
89 2010) have not been fully explored in an operational data assimilation system.

90 In this study, we develop a simple, computationally efficient, and effective data assimilation
91 approach for assimilating satellite soil moisture products into an operational national water
92 balance model. We demonstrate the application of the method to the Australian Water Resources
93 Assessment Community Modelling system (AWRA-CMS), which provides daily water balance
94 estimates at 5-km resolution across Australia, with the assimilation of satellite surface soil
95 moisture (SSM) from both SMOS and SMAP. A post-analysis adjustment is proposed to impart
96 mass conservation constraints on related states and fluxes such as root-zone soil water storage,
97 evapotranspiration and streamflow thus improving the accuracy of the water balance post
98 assimilation. The impacts of data assimilation on model predictions is assessed by quantifying
99 the persistence of the correction to key model components with respect to open-loop simulations.

100 **2 Materials and Methods**

101 2.1 Australian Water Resources Assessment Community Modelling system (AWRA-CMS)

102 The Australian Water Resources Assessment (AWRA) Community Modelling system (AWRA-
103 CMS) is a freely available version of the AWRA Landscape model (Van Dijk, 2010) which
104 simulates the water balance in the Australian landscape (https://github.com/awracms/awra_cms).
105 The operational implementation of the AWRA-CMS by the Australian Bureau of Meteorology
106 provides daily 0.05 degree (approximately 5 km) national gridded soil moisture, runoff,
107 evapotranspiration and deep drainage estimates, and underpins the annual national water
108 resource assessments and water use accounts (Frost et al., 2018) as well as providing situational
109 soil moisture for flood forecasting, agriculture and other applications. AWRA is a one-
110 dimensional distributed model that simulates the water balance for each grid cell across the
111 modelling domain by distributing rainfall into plant-accessible water, soil moisture and
112 groundwater stores, and removing water through evapotranspiration, runoff and deep drainage.
113 The soil water column has been partitioned into three layers (upper: 0–10 cm, lower: 10–100 cm,
114 and deep: 1–6 m) simulated separately for deep- and shallow-rooted vegetation. In addition to
115 the modelling of soil columns, the model includes a surface water and a groundwater storage that
116 are simulated at each grid cell and conceptualized as if operating within a small unimpaired
117 catchment. In this study, we used daily precipitation and air temperature from the gridded
118 climate data services (Jones et al., 2009), daily solar exposure produced from geostationary
119 satellites (Grant et al., 2008), and interpolated site-based wind speed (McVicar et al., 2008) as
120 model forcing inputs.

121 2.2 Satellite soil moisture (SSM)

122 To optimize the daily spatial coverage, we used two satellite soil moisture products derived from
123 passive L-band systems: the Soil Moisture Active-Passive (SMAP) product from NASA
124 (Entekhabi et al., 2010); and the product from the European Space Agency's (ESA's) Soil
125 Moisture and Ocean Salinity (SMOS) mission (Kerr et al., 2001). The SMAP product is the
126 level-2 enhanced radiometer half-orbit 9-km EASE-grid soil moisture (Chan et al., 2018). The
127 SMOS product is the level-2 soil moisture product on ~ 25-km grid (Rahmoune et al., 2013).
128 Both SMAP and SMOS produce volumetric soil moisture estimates (units m^3/m^3) of

129 approximately the upper 5 cm of soil. Available swath data for each product covering Australia
 130 were sourced and collated for 24-hour period approximating the AWRA-CMS operational time
 131 steps and interpolated to a regular 0.05-degree grid across the modelling domain from 2015 to
 132 2019. This provided maximum possible spatial coverage for each data product in representing
 133 surface soil moisture at the end of the model's time step integration each day.

134 2.3 Data assimilation approach through triple collocation (TC)

135 The data assimilation method used here is a time sequential updating of model state(s) given
 136 observations of relevant model variables (Reichle, 2008). Two key modelling components in
 137 data assimilation: the *dynamics operator*, which describes the time integration of the system
 138 states and fluxes, which in this study is the AWRA-CMS; and the *observation operator*, which
 139 provides the mathematical mapping from state to observation space (or vice versa). The role of
 140 the observation operator is to perform a mapping between observation and state space, as often
 141 observations are not directly comparable to model states.

142 The state updating equation for sequential data assimilation is written as:

$$143 \quad X_t^a = X_t^f + K_t[Y_t - H(X_t^f)] \quad (1)$$

144 which says that the best estimate of model state, known as analysis (X_t^a), is equal to the first
 145 guess or forecast (X_t^f) plus a weighted difference between observations, Y_t , and the model
 146 equivalent to the observation, $H(X_t^f)$, for that time step. The multiplier, K_t , is known as the *gain*
 147 *factor* which contains uncertainty expressed as error variance for both model estimates (σ_B^2) and
 148 observations σ_R^2 . For a unity observation operator and assuming independence between model
 149 estimates and observations, gain factor typically assumes the form:

$$150 \quad K = \frac{\sigma_B^2}{\sigma_B^2 + \sigma_R^2}. \quad (2)$$

151 In this study, the state variable of focus is the moisture storage in AWRA's upper soil layer, S_0 .
 152 Satellite surface soil moisture (SSM) products from both SMOS and SMAP are used as the
 153 observations to update the model simulation. Satellite soil moisture estimates are provided in
 154 volumetric units (m^3/m^3), whereas modeled upper-layer soil moisture is given in terms of

155 storage of water (i.e. units mm). The observation operator used here is a linear transformation
 156 which matches the mean and variance between model and observation time series (Tian et al.,
 157 2017). As such, the observation operator also simultaneously removes systematic bias between
 158 model estimates and satellite observations. In addition, for region with sparse rain-gauge
 159 coverage such as central Western Australia, the linear transformation of the satellite soil moisture
 160 products draws on data sampled from neighboring cells with similar soil moisture conditions, to
 161 account for known poor model estimates from consistent underestimation of rainfall (S1).

162 The gain factor, K , contains information on the error variances of the model and observations.
 163 Observation error variance is often estimated through field campaigns (Draper et al., 2009;
 164 Panciera et al., 2014), but these rarely represent the spatial and temporal variability of errors in
 165 gridded satellite products. Alternatively, data providers often specify error estimates, but their
 166 magnitude can be overly optimistic. Triple collocation (TC) was developed as a method of
 167 quantifying error characteristics in geophysical variables when the true error structure is elusive.
 168 It was first applied to near-surface wind data (Stoffelen, 1998) and later extensively applied to
 169 soil moisture (Dorigo et al., 2017; McColl et al., 2014; Scipal et al., 2008; Su et al., 2014) and
 170 rainfall (Massari et al., 2017). The assumption of this approach is that three independent data sets
 171 of the same geophysical variable can be used to infer the error variances in each. Here we use TC
 172 as a way of inferring error variances from our three independent estimates of surface soil
 173 moisture, AWRA S_0 , SMAP, and SMOS. McColl et al. (2014) shows that the error variances of
 174 each data set can be calculated from the temporal variance and covariance between data sets
 175 respectively as:

$$176 \quad \sigma_x^2 = \left(Q_{x,x} - \frac{Q_{x,y}Q_{x,z}}{Q_{y,z}} \right), \quad \sigma_y^2 = \left(Q_{y,y} - \frac{Q_{x,y}Q_{y,z}}{Q_{x,z}} \right) \quad \text{and} \quad \sigma_z^2 = \left(Q_{z,z} - \frac{Q_{z,y}Q_{x,z}}{Q_{x,y}} \right) \quad (3)$$

177 where x, y and z denote AWRA, SMAP or SMOS soil moisture estimates respectively and Q
 178 denotes temporal variance and covariance between the data sets. These estimates of the error

179 variances are then used in the determination of gain factors (Eq. 2) for the three estimates of soil
 180 moisture, thus recasting Equation (1) as:

$$181 \quad X_t^a = K_{AWRA} X_t^f + K_{SMAP} Y_t^{SMAP} + K_{SMOS} Y_t^{SMOS} \quad (4)$$

182 The analysed soil water state derived from Eq. (4) represents an optimal blending of AWRA S_0 ,
 183 SMAP and SMOS (S2).

184 2.4 Analysis increment redistribution (AIR)

185 The assimilation of satellite soil moisture often violates mass conservation in the model through
 186 the analysis update (Eq. 4). The difference between the analysis, X_t^a , and the forecast, X_t^f , (known
 187 as the *analysis increment*) represents an amount of water that has been added or subtracted from
 188 the system that was not present at the start of model integration for the given time step. In this
 189 study, we use the concept of tangent linear modelling (Errico, 1997; Giering, 2000) to
 190 redistribute the analysis increment of S_0 to all the relevant model states and fluxes (e.g. lower
 191 layer and deep layer soil water storage, evapotranspiration and runoff). This was considered as a
 192 way of maintaining mass (i.e. water) balance within a model time step, which data assimilation is
 193 known to break. We refer to this approach as analysis increment redistribution, or simply as AIR
 194 hereafter. To illustrate, Equation 5 gives an example of what should the resulting changes (Δ) in
 195 drainage (D_0) be, given the analysis increment in S_0 ($S_0^a - S_0^f$):

$$196 \quad \Delta D_0 = (1 - \beta_0) k_{0sat} \left[\left(\frac{S_0^a}{S_{0max}} \right)^2 - \left(\frac{S_0^f}{S_{0max}} \right)^2 \right], \quad (5)$$

197 where the k_{0sat} and S_{0max} are model parameters representing the saturated hydraulic
 198 conductivity and maximum storage of the upper soil layer, respectively, and β_0 is the
 199 proportion of upper soil layer lateral drainage (S3 for more detail). Corresponding adjustments
 200 of total lateral interflow for both upper and lower soil layer are then propagated to the river
 201 water storage and total runoff. In addition, the analysis increments of S_0 and change in lower
 202 soil layer water storage after application of the AIR are used to revise the total

203 evapotranspiration. The adjustments to the relevant states and fluxes are derived from AWRA
204 model formulation (S3).

205 2.5 In-situ measurements

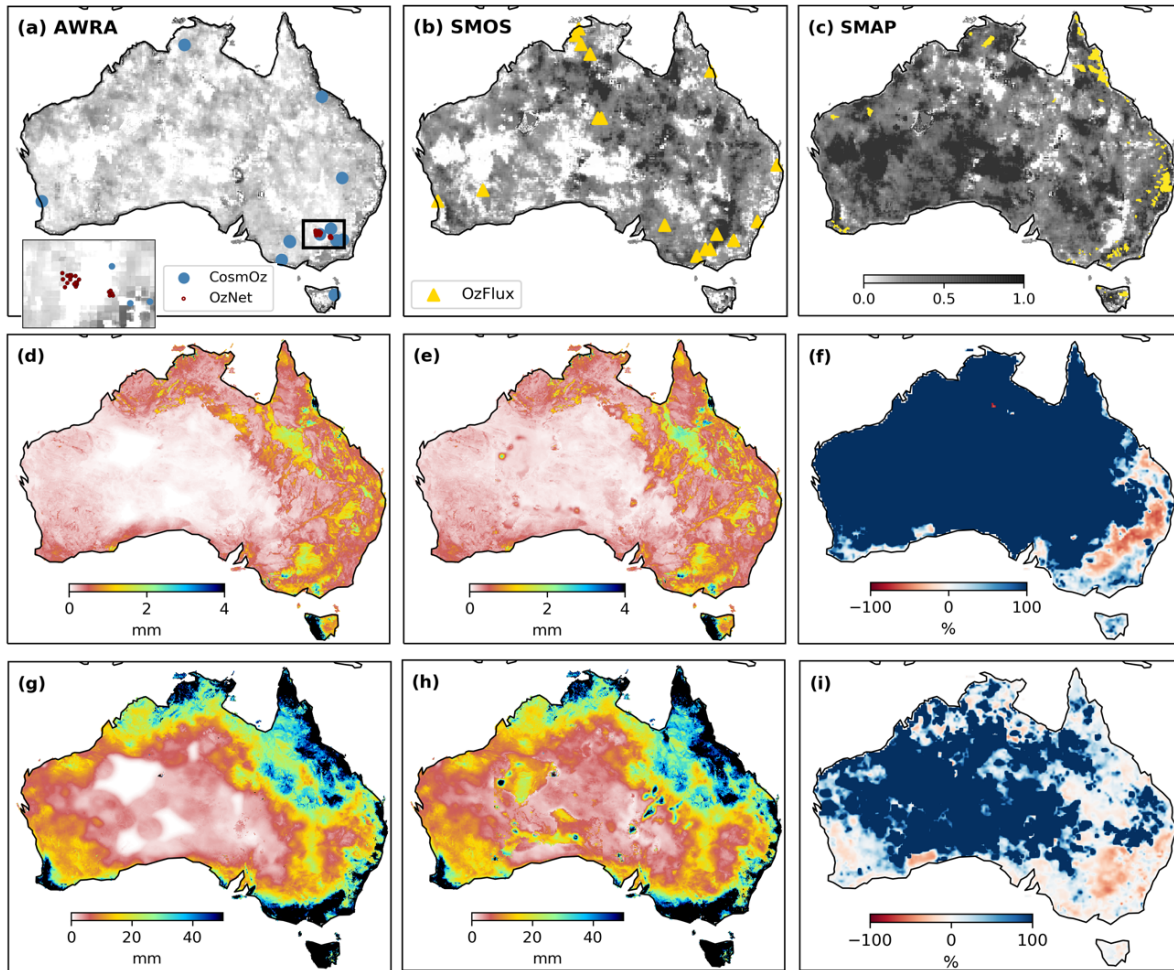
206 Evaluation of the modelled soil water storages was made against measurements from three soil
207 moisture monitoring networks in Australia from 2016 to 2018, namely OzNet (Smith et al.,
208 2012), CosmOz (Hawdon et al., 2014) (Fig. 1a) and OzFlux (Fig. 1b). AWRA model estimates
209 of upper layer soil water storage were compared against in situ measurements from the top 10 cm
210 of soil across all three networks. In situ measurements of root-zone moisture varied across
211 networks from 0-30 cm to 0-1 m. As such, AWRA soil water storages over the root-zone were
212 constructed accordingly by combining upper- and lower-layer soil water storage in the
213 appropriate proportions. OzFlux sites are primarily used for the evaluation of AWRA
214 evapotranspiration estimates, which were calculated from accumulated latent heat flux
215 measurements at each location. In total, there are 45 sites for soil moisture validation and 14 sites
216 for evapotranspiration validation. Streamflow observations for 100 catchments across Australia
217 have been used in the validation based on the quality and data availability (Fig. 1c).

218 2.6 Vegetation index

219 In water-limited regions like Australia, shallow-rooted vegetation normally responds quickly
220 with soil water availability, typically within a month. Consistency between root-zone soil water
221 storage and vegetation greenness may be considered as an indirect independent verification of
222 the simulation of root-zone soil water dynamic (Tian et al., 2019a; Tian et al., 2019b). The 0.05-
223 degree monthly Normalized Difference Vegetation Index (NDVI) from Moderate Resolution
224 Imaging Spectroradiometer (MODIS, MYD13C2 v6) is used to evaluate estimates of root-zone
225 soil moisture over cropland and grassland regions of the continent. The 250m land cover
226 classification map from Geoscience Australia (Lymburner et al. 2015) is resampled to 0.05
227 degree over model domain and used in the identification of crop and grassland cells.

228

229



230

231 **Figure 1** Study area showing gain factors of the TC data assimilation method rescaled to highlight relative contribution of the
 232 respective estimate: (a) AWRA-simulated S_0 , (b) SMOS soil moisture, and (c) SMAP soil moisture. Also displayed are the
 233 locations of in-situ monitoring stations from (a) CosmOz and OzNet networks, (b) OzFlux network, and (c) catchments for
 234 streamflow validation. Subfigures (d) and (e) are the average S_0 simulations for 2019 from AWRA open-loop (OL) and TC
 235 assimilation of SMOS and SMAP data (DA-TC). Subfigure (f) shows the average relative change of analysed S_0 (TC)
 236 compared to OL simulations in 2019. Subfigures (g) and (h) are the average S_s simulations for 2019 from AWRA OL and DA-TC.
 237 Subfigure (i) shows the average relative change of analysed S_s after analysis increment redistribution (TC-AIR) compared to OL
 238 simulations in 2019.

239

240 **3 Results and Discussion**

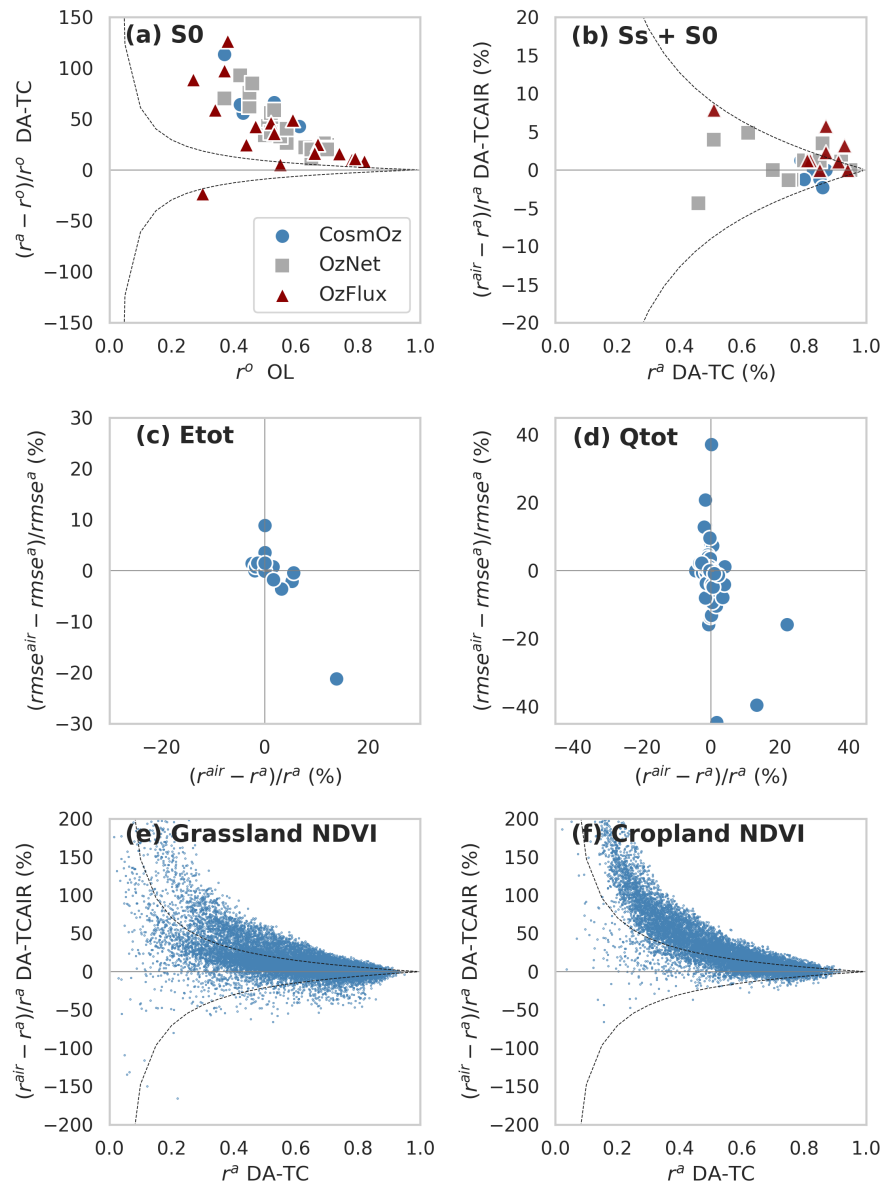
241 3.1 Improved spatial representation of soil moisture variability

242 The analysed upper layer soil water storage estimates receive a greater contribution from SSM
243 products, in particular SMAP observations, compared to model simulations (Figures 1a-c).
244 AWRA model simulations are driven by gauge-based rainfall analyses. As such they have
245 difficulty in adequately simulating soil moisture patterns over regions lacking in rain gauge
246 coverage, such as Western Australia and central Australia (Fig. 1d). Water storage simulations
247 over these regions default to zero, thus very little or no weight was given to the AWRA estimates
248 in these regions (Fig. 1a). In contrast, SMAP SSM data is heavily weighted in the assimilation
249 due to the smaller error variance derived from TC (Fig. 1c). This is expected since SMAP is the
250 best-performing satellite soil moisture product over the majority of applicable global land pixels
251 (Chen et al., 2018). AWRA simulations of S_0 are dominated by the satellite SSM data as a result
252 of TC data assimilation in the region which largely eliminates the erroneous artefacts associated
253 with deficient rainfall data forcing (Fig. 1e).

254 Moreover, the SSM data assimilation has the effect of adding moisture to AWRA S_0 simulations
255 over most of Australia, with predictions on average often in excess of 100% of those from the
256 OL simulations (Fig. 1f). The notable exception to this is in the southeast of Australia,
257 particularly within the Murray-Darling Basin, where SSM data assimilation reduced AWRA S_0
258 by more than 50%. This suggests that AWRA simulations underestimated the severity of the
259 drought experienced in the region in 2019.

260 TC assimilation only updates S_0 directly with satellite SSM, thus the S_s and other water storage
261 receives the impact from assimilation once the model integrates forward to the next time step
262 from the analysed S_0 as initial conditions. The AIR method adjusts S_s and other relevant states
263 and fluxes as a post-correction according to the change in S_0 to maintain water balance. The
264 average S_s with the correction in drainage and lateral interflow from the change in S_0 after TC
265 assimilation shows significant different spatial pattern with a relative change more than 100%

266 over those regions with sparse rain-gauge coverage against OL simulations (Fig. 1g-i, i.e. see the
 267 white regions in Fig1g in particular).



268

269 **Figure 2** Evaluation of AWRA-estimated upper soil water storage S_0 , root-zone soil water storage $S_s + S_0$, total
 270 evapotranspiration E_{tot} and runoff Q_{tot} : (a) relative change in correlation of S_0 from TC assimilation (DA-TC) compared to
 271 model open-loop (with dots above the zero line showing improved performance); (b) relative change in correlation of root-zone
 272 soil water storage from TC-AIR to DA-TC without mass redistribution; (c) – (d) relative correlation and RMSE changes in
 273 E_{tot} and Q_{tot} compared to DA-TC without AIR (with dots in the bottom right quadrant showing both improved correlation and
 274 reduced RMSE); (e) – (f) relative change in correlation between monthly root-zone soil water storage from TC-AIR with NDVI
 275 compared to DA-TC for all grid cells classified as grassland and cropland. Note that dashed curves delineate a 95% level of
 276 statistical significance.

277 3.2 Improved water balance estimates

278 Comparisons of AWRA simulations with and without SSM data assimilation were made against
279 in-situ measurements networks from 2016 to 2018. Consistent, statistically significant
280 improvement in modelled upper layer soil water storage estimates (S_0) was observed across all
281 sites (Fig. 2a) with the exception of a single OzFlux site located in a tropical rainforest, where
282 microwave SSM retrievals are typically poor in areas of dense vegetation (Njoku and Entekhabi,
283 1996). TC-based assimilation (Section 2.2) increases the correlation between in-situ surface SM
284 measurements from 0.47 to 0.72 on average for CosmOz sites, 0.54 to 0.69 for OzFlux sites, and
285 0.56 to 0.77 for OzNet sites compared to OL. This is a significant improvement in AWRA
286 simulations of surface soil moisture dynamics. Compared to ensemble methods of data
287 assimilation (e.g. Tian et al. 2017; 2019b) which rely on an initial guess of the error variance and
288 post hoc correction (e.g. inflation factors, Anderson, 2009), this proposed method based on TC is
289 simple, effective and computationally efficient, thus well suited to an operational system
290 simulating large-scale hydrology. Overall subtle improvements were observed across the AWRA
291 estimates of root-zone soil water storage, evapotranspiration and streamflow (results not shown,
292 see Tian et al., 2019c). The level of improvement is not surprising since those variables were not
293 directly updated with the TC assimilation and are only influenced through the integration of the
294 model to the next time step (Tian et al., 2019c).

295 The lack of water balance closure is arguably a weak point in data assimilation (Pan and Wood,
296 2006). Hence, we applied an analysis increments redistribution (AIR, Section 2.3) as a post-
297 correction to all relevant model states and fluxes to enforce mass conservation (water balance).
298 Although the absolute change S_0 is small relative to the volume of S_s , the corresponding change
299 in lower layer soil water storage is allocated through AIR based on model physics (S3). The
300 adjusted root-zone soil water storage (S_0+S_s) shows better agreement with in-situ measurements
301 by up to 10% compared to TC estimates without AIR (Fig. 2b). Improvements are found over the
302 majority of sites from OzFlux and OzNet with measurements. Improvements in correlation
303 together with reduced RMSE (Root-Mean-Squares Error) with in-situ measurements for E_{tot} are
304 found more than 10% relative to the TC estimates without AIR for some sites (Fig. 2c). Further
305 improvements in Q_{tot} simulations are found for some sites, with up to 40% reduction in RMSE
306 (Fig. 2d). Improvements in runoff simulation are due to, first, the SSM assimilation improving

307 pre-storm soil moisture status (Pauwels et al., 2001; Crow and Ryu, 2009), and then AIR adjusts
308 the interflow and river storage accordingly. This indicates the importance of accurate antecedent
309 soil moisture condition in the simulation of runoff response to subsequent rainfall.

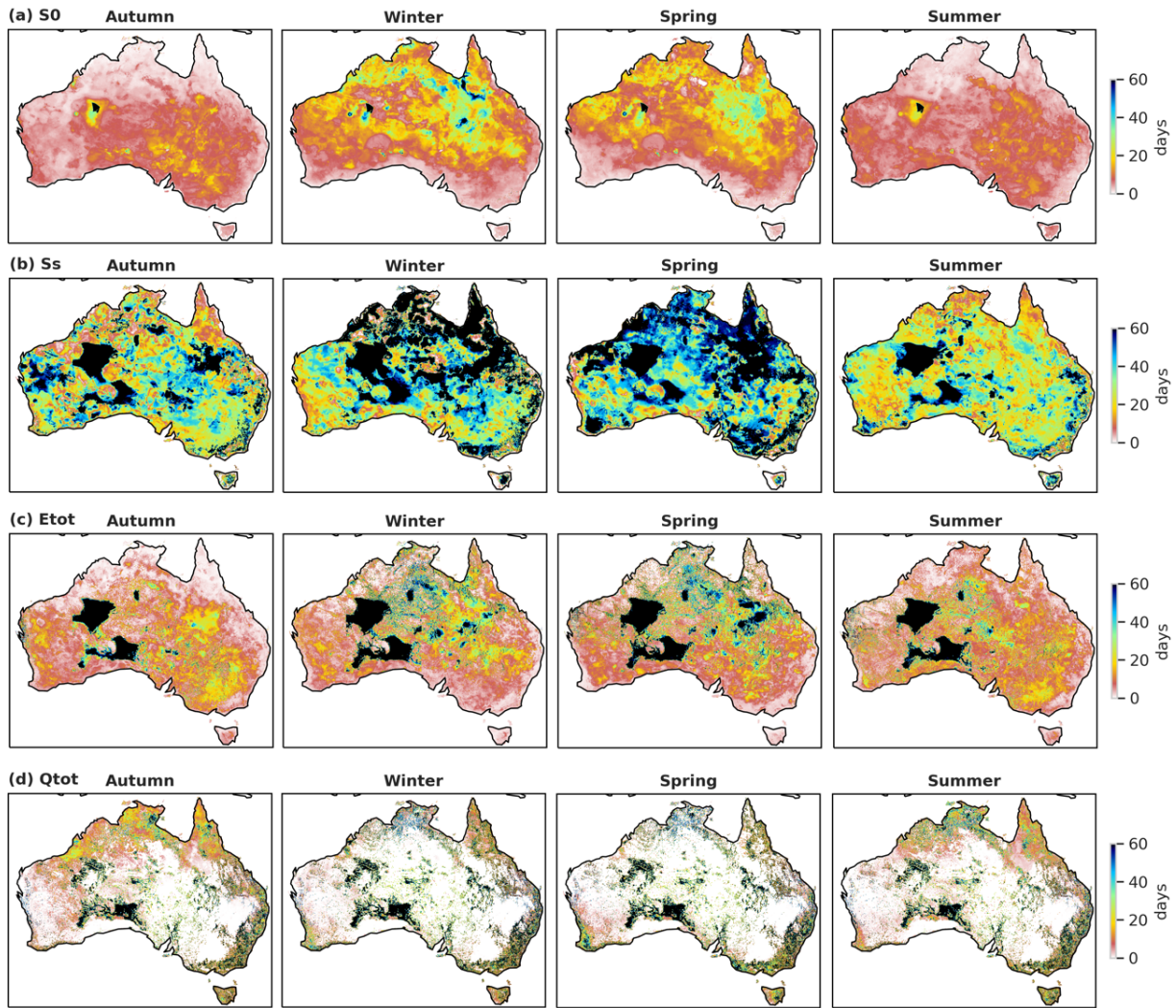
310 The inadequate distribution of in-situ observations as well as the large spatial disparity between
311 ground measurement and modelling scales are a great limitation for the evaluation of root-zone
312 soil moisture and evapotranspiration. AWRA simulation of root-zone soil moisture are compared
313 against satellite-derived NDVI in an indirect verification of model performance and as a way of
314 evaluating the impact of data assimilation. We calculated the correlation between time series of
315 monthly average AWRA root-zone soil moisture from OL, DA-TC and TC-AIR simulations
316 against NDVI for cropland and grassland of Australia over the period 2015 to 2018. These cover
317 types we selected as their rooting depths are commensurate with the combined soil depths of the
318 upper- and lower-soil water storages in AWRA. Figure 2e-f show the relative change in
319 correlation between root-zone simulations from DA-TC and those from TC-AIR data against
320 NDVI data for grassland and cropland areas of Australia. The figure shows that for the vast
321 majority of model grids, TC-AIR shows statistically significant increase in correlation with
322 NDVI compared to DA-TC alone, with an average increase in correlation with NDVI from 0.64
323 to 0.67 for grassland and 0.55 to 0.66 for cropland compared to OL. This demonstrates that
324 enforcing mass balances as part of the SSM data assimilation each time step is essential to
325 improving the simulation of root-zone soil water balance. The improved consistency with NDVI
326 also illuminates the potential of improving agricultural planning with more accurate information
327 of root-zone soil water availability.

328 3.3 Impacts on model predictions

329 Accurate soil water estimates can provide initial conditions for improved flood forecasting and
330 groundwater forecasting (Getirana et al., 2020a; Getirana et al., 2020b; Wanders et al., 2013).
331 Few studies quantify how long the impacts of data assimilation persist in the model system's
332 memory. In this study we used 100-day model simulations from initial states provided by the
333 AWRA OL and DA-TC with AIR. We calculated the number of days it took for the simulation
334 from the analysed DA-TCAIR states to converge to within +/- 5% of those from OL. The
335 experiments were run for one year from 1 March 2018 to 28 February 2019. Results show that
336 data assimilation can impact on model states and fluxes for weeks and sometimes up to 2-3

337 months (Fig. 3). The impacts of DA-TC with AIR can persist in simulated S_0 for as long as a
338 week over coastal regions, and longer in central Western Australia and Northern Australia with
339 up to 1 month persistence in winter and spring (Fig. 3a). There is less impact on S_0 simulations
340 during wet season since the S_0 can saturate rapidly due to the heavy rainfall. Overall, the longest
341 persistence is found in winter with a continental average of 13 days; the shortest persistence is 6
342 days on average in autumn and summer. The memory of initial conditions in simulations of S_s
343 can persist even longer due to the slower response to rainfall variability and higher field capacity.
344 Summer persistence for S_s is the least with a continental average of 30 days; in winter, this is
345 increased to 45 days.

346 Evapotranspiration estimates, however, do not feedback into the system and are highly variable
347 in time and space. On average, the impact of the antecedent soil moisture conditions on
348 evapotranspiration simulations can persist for 1 week over coastal areas, but up to months in
349 central Western Australia. The continental average varies from 13 to 20 days for each season.
350 The areas with the longest persistence are those areas with artefacts of zero rainfall in the
351 forcing. This demonstrates that improvements in AWRA estimates after SSM assimilation over
352 regions with sparse rain-gauge coverage can persist in the system for more than 2 months. The
353 impact on runoff varies from 1 week to 3 months over the continent. The majority of areas
354 impacted for more than 2 months are in locations of little rainfall and runoff. However, there
355 remains between 1-2 week impacts over north-eastern areas with heavy runoff.



356

357

358

359

360

361

Figure 3 Quantified impacts of data assimilation on forecasting AWRA state variables through the forecast of states for 100 days using the initial condition from DA-TCAIR: average time period that the impact of data assimilation can persist in autumn (2018.03-2018.05), Winter (2018.06-2018.08), Spring (2018.09-2018.11) and Summer (2018.12-2019.02) on (a) upper-layer soil water storage S_0 , (b) lower-layer soil water storage S_s , (c) total evapotranspiration E_{tot} and (d) total runoff Q_{tot} .

362 **4 Conclusion**

363 In this study, we proposed a simple and robust method for assimilating SMAP and SMOS soil
364 moisture products into the operational Australian Water Resources Assessment (AWRA) model.
365 The method involves the sequential (daily) updating of the model's upper layer soil water storage
366 with satellite soil moisture observations through a linear combination with weights determined
367 through triple collocation (DA-TC). Evaluation against in-situ measurements showed that
368 simulations of surface soil moisture dynamics is improved significantly after TC data
369 assimilation with an average increase of 0.23 correlation units compared with open-loop
370 simulations. Furthermore, we proposed an additional component to the data assimilation
371 whereby the analysis increment of the upper layer soil water storage is propagated into relevant
372 model states and fluxes as a way of maintaining mass balance (TC-AIR). An evaluation of the
373 root-zone soil moisture, evapotranspiration and streamflow estimates showed that the TC-AIR
374 appeared to only provide marginal, yet positive, improvement over the TC data assimilation
375 method alone. However, in an indirect verification of modelled root-zone soil moisture against
376 satellite-derived NDVI, TC-AIR was seen to provide significant improvement on TC method
377 alone. This demonstrates that by enforcing mass balances as part of the SSM data assimilation
378 each time step, AWRA can better represent soil water dynamics with greater consistency with
379 vegetation response.

380
381 The assimilation of satellite soil moisture estimates together with the mass redistribution reduces
382 the uncertainties in model estimates resulting mainly from uncertain forcing and model physics,
383 and provides temporally and spatially varying constraints on model water balance estimates. For
384 example, the assimilation resolves the gaps in rainfall forcing, and the underestimate of drought
385 condition over south-eastern areas in 2019. We demonstrate that the impacts of data assimilation
386 can persist in the model system for more than a week for surface soil water storage and more
387 than a month for root-zone soil water storage. This highlights the importance of accurate initial
388 hydrological states for improving forecast skill over longer lead times. Hence, an operational
389 water balance modelling system, with satellite data assimilation, has strong potential to add value
390 for assessing and predicting water availability for a range of decisions across industries and
391 sectors.

392 Acknowledgments

393 This project is supported by collaborative research agreement between the Australian Bureau of
394 Meteorology and Australian National University. We would like to thank Stuart Baron-Hay from
395 the Bureau of Meteorology for his help with implementation of the in AWRA-CMS. This
396 research was undertaken with the assistance of resources and services from the National
397 Computational Infrastructure (NCI), which is supported by the Australian Government through
398 the National Collaborative Research Infrastructure Strategy.

399 Data Availability

400 The AWRA-CMS code is accessible from github (https://github.com/awracms/awra_cms).
401 SMAP product used here is the level-2 enhanced radiometer half-orbit 9-km EASE-grid soil
402 moisture from the US National Snow and Ice Data Center (<https://nsidc.org>). SMOS level-2 soil
403 moisture product is available from ESA's SMOS online dissemination service ([https://smos-
404 diss.eo.esa.int/oads/access/](https://smos-diss.eo.esa.int/oads/access/)). The MYD13C2 NDVI data is accessible through Land Processes
405 Distributed Active Archive Centre (<https://lpdaac.usgs.gov>). The National Dynamic Land Cover
406 Dataset of Australia is available from Geoscience Australia (<https://www.ga.gov.au>).

407 References

- 408 Chan, S. K., Bindlish, R., O'Neill, P., Jackson, T., Njoku, E., Dunbar, S., et al. (2018).
409 Development and assessment of the SMAP enhanced passive soil moisture product. *Remote*
410 *Sensing of Environment*, 204, 931-941.
- 411 Chen, F., Crow, W. T., Bindlish, R., Colliander, A., Burgin, M. S., Asanuma, J., & Aida, K.
412 (2018). Global-scale evaluation of SMAP, SMOS and ASCAT soil moisture products using
413 triple collocation. *Remote Sensing of Environment*, 214, 1-13
- 414 Crow, W. T., & Ryu, D. (2009). A new data assimilation approach for improving runoff
415 prediction using remotely-sensed soil moisture retrievals. *Hydrology and Earth System Sciences*,
416 13(1), 1-16.
- 417 Davies, T., Cullen, M. J. P., Malcolm, A. J., Mawson, M. H., Staniforth, A., White, A. A., &
418 Wood, N. (2005). A new dynamical core for the Met Office's global and regional modelling of
419 the atmosphere. *Quarterly Journal of the Royal Meteorological Society*, 131(608), 1759-1782.
- 420 de Rosnay, P., Drusch, M., Vasiljevic, D., Balsamo, G., Albergel, C., & Isaksen, L. (2013). A
421 simplified Extended Kalman Filter for the global operational soil moisture analysis at ECMWF.
422 *Quarterly Journal of the Royal Meteorological Society*, 139(674), 1199-1213.
- 423 Dharssi, I., Bovis, K. J., Macpherson, B., & Jones, C. P. (2011). Operational assimilation of
424 ASCAT surface soil wetness at the Met Office. *Hydrology and Earth System Sciences*, 15(8),
425 2729-2746.

- 426 Dorigo, W., Wagner, W., Albergel, C., Albrecht, F., Balsamo, G., Brocca, L., et al. (2017). ESA
427 CCI Soil Moisture for improved Earth system understanding: State-of-the art and future
428 directions. *Remote Sensing of Environment*, 203, 185-215.
- 429 Draper, C. S., Reichle, R. H., De Lannoy, G. J. M., & Liu, Q. (2012). Assimilation of passive
430 and active microwave soil moisture retrievals. *Geophysical Research Letters*, 39.
- 431 Draper, C. S., Walker, J. P., Steinle, P. J., de Jeu, R. A. M., & Holmes, T. R. H. (2009). An
432 evaluation of AMSR-E derived soil moisture over Australia. *Remote Sensing of Environment*,
433 113(4), 703-710.
- 434 Lymburner, L., Tan, P., McIntyre, A., Thankappan, M., Sixsmith, J. (2015). Dynamic Land
435 Cover Dataset Version 2.1. Geoscience Australia, Canberra.
436 <http://pid.geoscience.gov.au/dataset/ga/83868>
- 437 Entekhabi, D., Njoku, E. G., O'Neill, P. E., Kellogg, K. H., Crow, W. T., Edelstein, W. N., et al.
438 (2010). The Soil Moisture Active Passive (SMAP) Mission. *Proceedings of the Ieee*, 98(5), 704-
439 716.
- 440 Errico, R. M. (1997). What is an adjoint model?. *Bulletin of the American Meteorological*
441 *Society*, 78(11), 2577-2592.
- 442 Frost, A., A. Ramchurn, and A. Smith (2018). The Australian Landscape Water Balance model
443 (AWRA-L v6), Technical Description of the Australian Water Resources Assessment Landscape
444 model version 6. *Bureau of Meteorology Technical Report*, Canberra: Bureau of Meteorology.
- 445 Getirana, A., Rodell, M., Kumar, S., Beaudoin, H. K., Arsenault, K., Zaitchik, B., et al. (2020).
446 GRACE Improves Seasonal Groundwater Forecast Initialization over the United States. *Journal*
447 *of Hydrometeorology*, 21(1), 59-71.
- 448 Getirana, A., Jung, H. C., Arsenault, K., Shukla, S., Kumar, S., Peters-Lidard, C., et al. (2020).
449 Satellite Gravimetry Improves Seasonal Streamflow Forecast Initialization in Africa. *Water*
450 *Resources Research*, 56(2), doi: 10.1029/2019wr026259.
- 451 Giering, R. (2000). Tangent linear and adjoint biogeochemical models. *Inverse Methods in*
452 *Global Biogeochemical Cycles*, 114, 33-48.
- 453 Grant, I., Jones, D., Wang, W., Fawcett, R., and Barratt, D. (2008). Meteorological and remotely
454 sensed datasets for hydrological modelling: A contribution to the Australian Water Availability
455 Project, paper presented at Catchment-scale Hydrological Modelling and Data Assimilation
456 (CAHMDA-3). *International Workshop on Hydrological Prediction: Modelling, Observation*
457 *and Data Assimilation*, Melbourne, Citeseer.
- 458 Hawdon, A., McJannet, D., & Wallace, J. (2014). Calibration and correction procedures for
459 cosmic-ray neutron soil moisture probes located across Australia. *Water Resources Research*,
460 50(6), 5029-5043.
- 461 Ines, A. V. M., Das, N. N., Hansen, J. W., & Njoku, E. G. (2013). Assimilation of remotely
462 sensed soil moisture and vegetation with a crop simulation model for maize yield prediction.
463 *Remote Sensing of Environment*, 138, 149-164.
- 464 Jones, D. A., Wang, W., & Fawcett, R. (2009). High-quality spatial climate data-sets for
465 Australia. *Australian Meteorological and Oceanographic Journal*, 58(4), 233-248.

- 466 Kerr, Y. H., Waldteufel, P., Wigneron, J. P., Martinuzzi, J. M., Font, J., & Berger, M. (2001).
467 Soil moisture retrieval from space: The Soil Moisture and Ocean Salinity (SMOS) mission. *Ieee*
468 *Transactions on Geoscience and Remote Sensing*, 39(8), 1729-1735.
- 469 Koster, R. D., Dirmeyer, P. A., Guo, Z. C., Bonan, G., Chan, E., Cox, P., et al. (2004). Regions
470 of strong coupling between soil moisture and precipitation. *Science*, 305(5687), 1138-1140.
- 471 Massari, C., Crow, W., & Brocca, L. (2017). An assessment of the performance of global rainfall
472 estimates without ground-based observations. *Hydrology and Earth System Sciences*, 21(9),
473 4347-4361.
- 474 McColl, K. A., Vogelzang, J., Konings, A. G., Entekhabi, D., Piles, M., & Stoffelen, A. (2014).
475 Extended triple collocation: Estimating errors and correlation coefficients with respect to an
476 unknown target. *Geophysical Research Letters*, 41(17), 6229-6236.
- 477 McVicar, T. R., Van Niel, T. G., Li, L. T., Roderick, M. L., Rayner, D. P., Ricciardulli, L., &
478 Donohue, R. J. (2008). Wind speed climatology and trends for Australia, 1975-2006: Capturing
479 the stilling phenomenon and comparison with near-surface reanalysis output. *Geophysical*
480 *Research Letters*, 35(20)
- 481 Njoku, E. G., & Entekhabi, D. (1996). Passive microwave remote sensing of soil moisture.
482 *Journal of Hydrology*, 184(1-2), 101-129.
- 483 Pan, M., & Wood, E. F. (2006). Data assimilation for estimating the terrestrial water budget
484 using a constrained ensemble Kalman filter. *Journal of Hydrometeorology*, 7(3), 534-547.
- 485 Panciera, R., Walker, J. P., Jackson, T. J., Gray, D. A., Tanase, M. A., Ryu, D., et al. (2014). The
486 Soil Moisture Active Passive Experiments (SMAPEX): Toward Soil Moisture Retrieval From the
487 SMAP Mission. *Ieee Transactions on Geoscience and Remote Sensing*, 52(1), 490-507.
- 488 Pauwels, V. R. N., Hoeben, R., Verhoest, N. E. C., & De Troch, F. P. (2001). The importance of
489 the spatial patterns of remotely sensed soil moisture in the improvement of discharge predictions
490 for small-scale basins through data assimilation. *Journal of Hydrology*, 251(1-2), 88-102.
- 491 Pipunic, R. C., Walker, J. P., & Western, A. (2008). Assimilation of remotely sensed data for
492 improved latent and sensible heat flux prediction: A comparative synthetic study. *Remote*
493 *Sensing of Environment*, 112(4), 1295-1305.
- 494 Rahmoune, R., Ferrazzoli, P., Kerr, Y. H., & Richaume, P. (2013). SMOS Level 2 Retrieval
495 Algorithm Over Forests: Description and Generation of Global Maps. *Ieee Journal of Selected*
496 *Topics in Applied Earth Observations and Remote Sensing*, 6(3), 1430-1439.
- 497 Reichle, R. H., & Koster, R. D. (2005). Global assimilation of satellite surface soil moisture
498 retrievals into the NASA Catchment land surface model. *Geophysical Research Letters*, 32(2).
499 <https://doi.org/10.1016/j.advwatres.2008.01.001>
- 500 Reichle, R. H. (2008). Data assimilation methods in the Earth sciences. *Advances in Water*
501 *Resources*, 31(11), 1411-1418.
- 502 Renzullo, L. J., van Dijk, A. I. J. M., Perraud, J. M., Collins, D., Henderson, B., Jin, H., et al.
503 (2014). Continental satellite soil moisture data assimilation improves root-zone moisture analysis
504 for water resources assessment. *Journal of Hydrology*, 519, 2747-2762.

- 505 Scipal, K., Drusch, M. & Wagner, W., (2008). Assimilation of a ERS scatterometer derived soil
506 moisture index in the ECMWF numerical weather prediction system, *Advances in water*
507 *resources*, 31(8), 1101-1112.
- 508 Sheffield, J., & Wood, E. F. (2007). Characteristics of global and regional drought, 1950-2000:
509 Analysis of soil moisture data from off-line simulation of the terrestrial hydrologic cycle.
510 *Journal of Geophysical Research-Atmospheres*, 112(D17).
- 511 Smith, A. B., Walker, J. P., Western, A. W., Young, R. I., Ellett, K. M., Pipunic, R. C., et al.
512 (2012). The Murrumbidgee soil moisture monitoring network data set. *Water Resources*
513 *Research*, 48.
- 514 Stoffelen, A. (1998). Toward the true near-surface wind speed: Error modeling and calibration
515 using triple collocation. *Journal of Geophysical Research-Oceans*, 103(C4), 7755-7766.
- 516 Su, C. H., Ryu, D., Crow, W. T., & Western, A. W. (2014). Beyond triple collocation:
517 Applications to soil moisture monitoring. *Journal of Geophysical Research-Atmospheres*,
518 119(11), 6419-6439.
- 519 Tian, S., van Dijk, A. I. J. M., Tregoning, P., & Renzullo, L. J. (2019). Forecasting dryland
520 vegetation condition months in advance through satellite data assimilation. *Nature*
521 *Communications*, 10. (1), 1-7.
- 522 Tian, S., Tregoning, P., Renzullo, L. J., van Dijk, A. I. J. M., Walker, J. P., Pauwels, V. R. N., &
523 Allgeyer, S. (2017). Improved water balance component estimates through joint assimilation of
524 GRACE water storage and SMOS soil moisture retrievals. *Water Resources Research*, 53(3),
525 1820-1840.
- 526 Tian, S., Renzullo, L. J., van Dijk, A. I. J. M., Tregoning, P., & Walker, J. P. (2019). Global joint
527 assimilation of GRACE and SMOS for improved estimation of root-zone soil moisture and
528 vegetation response. *Hydrology and Earth System Sciences*, 23(2), 1067-1081.
- 529 Tian, S., Renzullo, L. J., Pipunic, R., Sharples, W., Lerat, J., & Donnelly, C.(2019),.
530 Assimilating satellite soil moisture retrievals to improve operational water balance modelling.
531 *Proceedings of the 23rd International Congress on Modelling and Simulation*, Canberra,
532 Australia. <https://doi.org/10.36334/modsim.2019.H6.tian>
- 533 van Dijk, A.I.J.M. (2010). AWRA Technical Report 3, Landscape Model (version 0.5) Technical
534 Description, WIRADA, Canberra: CSIRO Water for a Healthy Country Flagship.
- 535 Vinnikov, K. Y., Robock, A., Speranskaya, N. A., & Schlosser, A. (1996). Scales of temporal
536 and spatial variability of midlatitude soil moisture. *Journal of Geophysical Research-*
537 *Atmospheres*, 101(D3), 7163-7174.
- 538 Wanders, N., Karssenber, D., de Roo, A., de Jong, S. M., & Bierkens, M. F. P. (2014). The
539 suitability of remotely sensed soil moisture for improving operational flood forecasting.
540 *Hydrology and Earth System Sciences*, 18(6), 2343-2357.